Journal of
Materials Chemistry

Cite this: *J. Mater. Chem.*, 2012, **22**, 15620

www.rsc.org/materials

PAPER

Peripheral modification of 1,3,5-triazine based electron-transporting host materials for sky blue, green, yellow, red, and white electrophosphorescent devices†

Hsiao-Fan Chen,[a] Ting-Chih Wang,[a] Shih-Wei Lin,[a] Wen-Yi Hung,*[b] Hung-Chi Dai,[b] Hao-Chih Chiu,[b] Ken-Tsung Wong,*[a] Meng-Huan Ho,[c] Ting-Yi Cho,[c] Chieh-Wei Chen[c] and Chung-Chun Lee[c]

Received 27th March 2012, Accepted 7th June 2012
DOI: 10.1039/c2jm31904g

A systematic comparison of the physical properties and the dual-role (host and electron transport) applications of star-shaped 1,3,5-triazine-based ET-type hosts (**T2T**, **3N-T2T**, **3P-T2T**, and ***o*CF3-T2T**) with differential peripheral groups was reported. The introduction of *N*-heterocyclic polar peripheries onto a 1,3,5-triazine core gave evident benefits to the electron injection/transport properties, rendering efficient PhOLEDs with a simpler device configuration feasible. Among these hosts, **3P-T2T** can serve both as a promising host and electron-transport material for various Ir-based electrophosphorescence devices. These PhOLEDs configured with the same device structure exhibited low operation voltages with a maximum η_{ext} of 8%, 15.7%, 16.9%, 16.4% and 10.8% for sky blue (FIrpic), green [$(PPy)_2Ir(acac)$], yellow [$(Bt)_2Ir(acac)$], red [$(Mpq)_2Ir(acac)$] and white [FIrpic + 0.5 wt% $(Mpq)_2Ir(acac)$], respectively.

Introduction

Phosphorescent light-emitting devices (PhOLEDs) have received great attention for over a decade because they can effectively harvest electro-generated singlet and triplet excitons to achieve a theoretical 100% internal quantum efficiency.[1] One common strategy utilized to obtain highly efficient PhOLEDs is to suppress the detrimental effects of transition metal-centered phosphors, such as aggregation quenching (triplet–triplet annihilation), by adapting suitable host materials.[2] Usually, the criteria for suitable host materials are (i) a higher triplet energy than that of the guest molecule to prevent exothermic reverse energy transfer enabling triplet excitons to be effectively confined within the emitting layer;[3] (ii) appropriately aligned energy levels relative to those of the neighboring active layers for better charge injection, giving devices with low operating voltage; (iii) excellent and balanced charge carrier transport properties to increase charge flux and thus enhance the propensity for electron–hole recombination, rendering high efficiency. Typically, the device configuration of an efficient PhOLED comprising a judicious selection of active materials is very sophisticated, impeding the reduction of production costs. One of the possible solutions is to design bifunctional host molecules. For example, host materials with a preference for hole-transport (HT)[4] or electron-transport (ET)[5–7] are of great potential to achieve cost-effective PhOLEDs. The advantage of using such host materials is that the device can be free of a hole-transport layer (HTL) or an electron-transport layer (ETL). This strategy will reduce the complications of device fabrication and thus is beneficial to lower the production costs. Along this line, some interesting host materials capable of transporting electrons have been developed and have served the dual-role of host as well as ETL.[6] In addition to those excellent examples, we have previously reported a series of 1,3,5-triazine-based ET-type hosts for PhOLEDs.[7] With **T2T** (Scheme 1) as the host for green phosphor, $(PPy)_2Ir(acac)$, and TPBI as the ETL, the PhOLED exhibited an external quantum efficiency and power efficiency of 17.5% and 59 lm W^{-1}, respectively. Since **T2T** possesses good electron mobility ($\mu_e = 1.2 \times 10^{-4}$ cm^2 V^{-1} s^{-1}), it was reasonably utilized as an ET material. However, the device efficiencies dropped greatly (9.7% and 14.7 lm W^{-1}) as **T2T** was used to replace the typical ET material TBPI. This result indicated that the ET and/or electron injection ability of **T2T** is insufficiently good despite its high electron mobility. Taking the advantage of the high electron mobility of 1,3,5-triazine-centered molecules, we report herein our peripherally modified 1,3,5-triazine-based ET-type hosts by incorporating different polar aromatic groups, namely 1-pyrazolyl and *o*-trifluorophenyl, onto the three *meta*-positions of C_3-symmetry 2,4,6-triphenyl-1,3,5-triazine, giving **3P-T2T** and ***o*CF3-T2T**, respectively. Another heteroarene (2-pyridyl) substituted counterpart, (**3N-T2T**),[5]

---

[a] *Department of Chemistry, National Taiwan University, Taipei 10617, Taiwan. E-mail: kenwong@ntu.edu.tw; Fax: +886 2 33661667; Tel: +886 2 33661665*
[b] *Institute of Optoelectronic Sciences, National Taiwan Ocean University, Keelung, 20224, Taiwan. E-mail: wenhung@mail.ntou.edu.tw*
[c] *Advanced Research Center, AU Optronics, Science-Based Industrial Park, Hsinchu 30078, Taiwan*

† Electronic supplementary information (ESI) available. See DOI: 10.1039/c2jm31904g

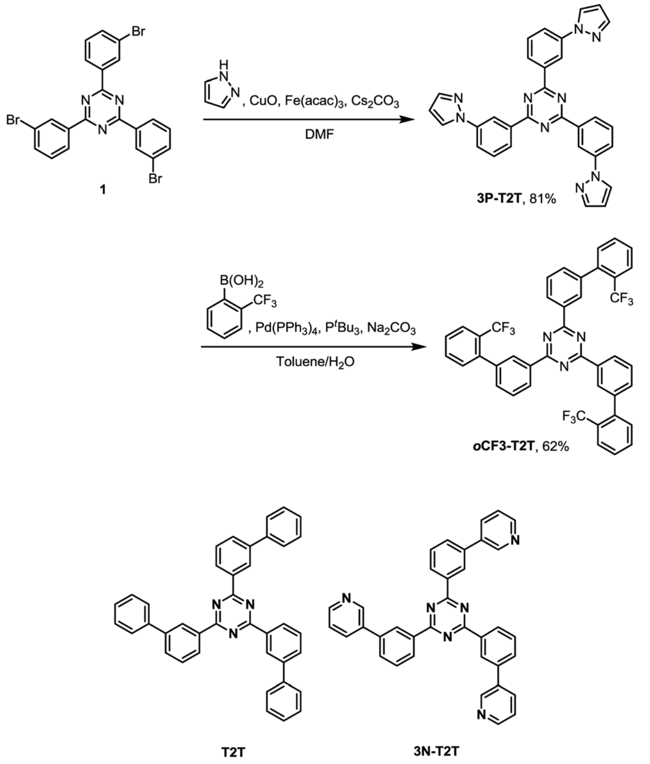

Scheme 1 Synthesis of **3P-T2T** and ***o*CF3-T2T** and the chemical structures of **T2T** and **3N-T2T**.

firstly reported by Kido *et al.* was also included in this contribution for comparison. We anticipated that the introduction of different aryl groups would allow the fine-tuning of the photophysical properties, triplet energies, energy levels, and electron transport properties. We discovered that **3P-T2T** can serve as a universal host for various heavy metal-containing RGB phosphors as well as an efficient electron-transport material, giving electrophosphorescence with remarkable efficiencies. The devices using **3P-T2T** as host and ETL achieved maximum external quantum efficiencies (η_{ext}) up to 7.8% (3.7 V) for sky blue, 15% (4.1 V) for green, 16.5% (4.1 V) for yellow, and 13.7% (4.6 V) for red-emitting PhOLEDs. In addition, a two-emitter based white OLED utilizing an ET-type host **3P-T2T** achieved a maximum η_{ext} of 10.5%. The practical uses of ET-type hosts in various PhOLEDs were successfully demonstrated, giving devices with high quantum efficiencies and low operating voltages at high brightness even without using a complicated p–i–n junction technique.

Results and discussion

Synthesis

Scheme 1 depicts the synthetic pathway toward new 1,3,5-triazine-based ET-type host molecules, **3P-T2T** and ***o*CF3-T2T**. The bromo-substituted 1,3,5-triazine intermediate **1** was obtained according to our previous report.[7] The C–N bond formation between 1*H*-pyrazole and **1** catalyzed by a copper/iron co-catalyst gave **3P-T2T** with 81% yield.[8] ***o*CF3-T2T** was synthesized in 62% yield *via* Suzuki-coupling of 2-(trifluoromethyl)phenylboronic acid[9] and **1**.

Thermal properties

The morphological properties and thermal stabilities of **3N-T2T**, **3P-T2T**, and ***o*CF3-T2T** were studied by differential scanning calorimetry (DSC) and thermogravimetric analysis (TGA), respectively. The data, together with previously reported **T2T**, are summarized in Table 1. Notably, due to the highly twisted nature, ***o*CF3-T2T** only exhibited a well-defined glass transition temperature (T_g) at 75 °C in the DSC scan up to 400 °C. In contrast, **3N-T2T** and **3P-T2T** showed no distinct phase transition below their melting points of 391 and 352 °C, respectively. The variation of their morphological properties might be closely related to the different electronic natures of the molecules imparted by the polar peripheral substituents. Compounds **3N-T2T**, **3P-T2T**, and ***o*CF3-T2T** showed good thermal stabilities with decomposition temperatures (T_d, corresponding to 5% weight loss) in the range of 313–391 °C. A high durability toward temperature is desirable for host materials in PhOLEDs because it prevents morphological changes and suppresses the formation of aggregates upon heating.

Photophysical and electrochemical properties

Fig. 1 presents the UV-visible absorption and photoluminescence (PL) spectra of the solutions (CH_2Cl_2) and solid thin films. The photophysical data are summarized in Table 1. In solution, all compounds exhibited similar absorption maxima in a range of 266–274 nm while broadened spectra were observed in the solid thin films, presumably due to the different dielectric surroundings in the solid state. The similar absorption maxima indicate that the different peripheries do not significantly alter the effective conjugation.

Compounds **3N-T2T**, **3P-T2T**, and ***o*CF3-T2T** exhibited deep blue emissions in CH_2Cl_2 solutions with PL peaks located in the range 374–409 nm. In thin films, no emission was detected for **3N-T2T**, **3P-T2T**, and ***o*CF3-T2T**, indicating that self-quenching is severely enhanced by polar peripheries. The triplet energies (E_T) of **3N-T2T**, **3P-T2T**, and ***o*CF3-T2T** were calculated as 2.82, 2.80, and 2.79 eV, respectively, referring to the highest energy vibronic sub-band of the phosphorescence spectra measured at 77 K (EtOH). The high triplet energies of these host materials suggest their suitability for hosting various RGB phosphors. The electrochemical properties of **T2T**, **3N-T2T**, **3P-T2T**, and ***o*CF3-T2T** were examined by cyclic voltammetry (CV) as shown in Fig. 2. The measurements were performed in THF with ferrocene as the internal reference. All compounds exhibited reversible reduction peaks which can be unambiguously assigned to the reductions of 1,3,5-triazine cores. LUMO levels were obtained from reduction potentials using published correlations,[10] whereas HOMO levels were calculated *via* HOMO = LUMO − $E_{transport}$ (where $E_{transport}$ is the transport gap energy, obtained from the optical gap with published correlation[9]). **3N-T2T**, **3P-T2T**, and ***o*CF3-T2T** possess slightly stabilized LUMO levels as compared with that of **T2T**, indicating the electron-withdrawing nature of the peripheral substituents.

Table 1 Physical properties of **T2T**, **3N-T2T**, **3P-T2T**, and ***o*CF3-T2T**

	$T_g/T_c/T_m$ (°C)	T_d (°C)	$E_{1/2}^{\mathrm{Red}a}$ (V)	λ_{abs} (nm) [sol./film]	$\lambda_{\mathrm{PL}}{}^{b}$ (nm) [sol./film]	E_T (eV)	$E_g{}^{c}$ (eV)	HOMO/LUMO^d/$E_{\mathrm{transport}}$ (eV)
T2T	95/137/204	352	−2.13	270/270	380/400	2.80	3.56	−6.74/−2.25/4.49
3N-T2T	n.d.^{e}/n.d./255	391	−2.08	274/277	359, 374/n.d.	2.82	3.55	−6.77/−2.30/4.47
3P-T2T	n.d./n.d./250	352	−2.06	266/268	395/n.d.	2.80	3.45	−6.67/−2.33/4.34
***o*CF3-T2T**	75/n.d./n.d.	313	−2.04	274/276	409/n.d.	2.79	3.55	−6.82/−2.35/4.47

[a] Reduction potential *vs.* ferrocene/ferrocenium redox couple. [b] The excitation wavelength was set to the absorption maximum. [c] Calculated from the absorption onset of the solid film. [d] LUMO energy level calculated from the reduction potential with published correlation. HOMO = LUMO − $E_{\mathrm{transport}}$, where $E_{\mathrm{transport}}$ is obtained from E_g with published correlation. [e] Not detected.

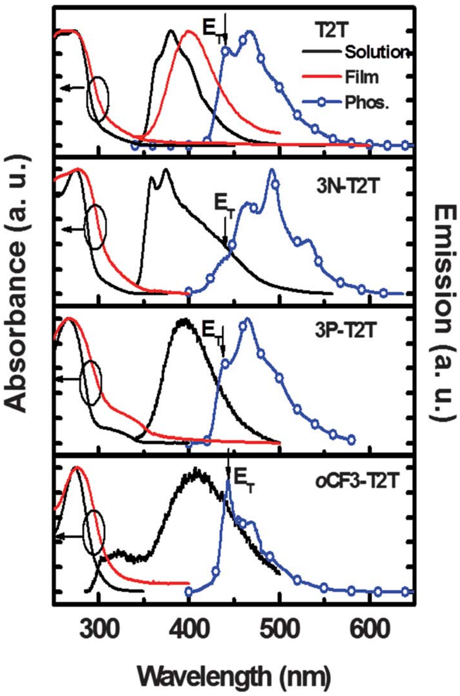

Fig. 1 Room-temperature absorption and emission (PL) spectra of **T2T**, **3N-T2T**, **3P-T2T**, and ***o*CF3-T2T** in CH_2Cl_2 solutions and as neat films and the corresponding phosphorescence (Phos) spectra recorded from their EtOH solutions at 77 K.

Electron transport

T2T showed excellent electron mobility [$\mu_e = 1.2 \times 10^{-4}$ cm^2 V^{-1}s^{-1}, determined by time-of-flight (TOF) technique][7] which is 10-fold higher than that of the widely used ET material tris(8-hydroxyquinoline) aluminium (Alq_3). We attempted to acquire the electron mobilities of **3N-T2T**, **3P-T2T**, and ***o*CF3-T2T** *via* the TOF technique. However, we could not observe transient photocurrent signals to evaluate their electron mobilities. Therefore, we fabricated electron-only devices with a device structure of ITO/BCP (30 nm)/compound (50 nm)/LiF/Al to investigate the electron-transport behaviour. Fig. 3 depicts the current *vs.* voltage characteristics of the electron-only devices. The introduction of BCP on top of ITO is to limit the injection of hole carriers. Surprisingly, the turn-on voltages for the devices with a **3N-T2T** or **3P-T2T** host were almost half those of the **T2T**-based devices. The noteworthy decreases in driving voltages indicate that **3N-T2T** and **3P-T2T** are even more efficient for electron-transport and/or injection than **T2T**, which has been shown to have high electron mobility in our previous study. The great improvement of the electron-transport properties of **3N-T2T** and **3P-T2T** is attributed to the introduction of *N*-heterocyclic polar peripheries, pyridyl or pyrazolyl groups, which are known as electron-withdrawing heteroaromatic groups. However, simply attaching –CF_3 to the outer phenylene rings (***o*CF3-T2T**) did not present any improvement in the electron-only device, indicating that the introduction of *N*-heteroarene is

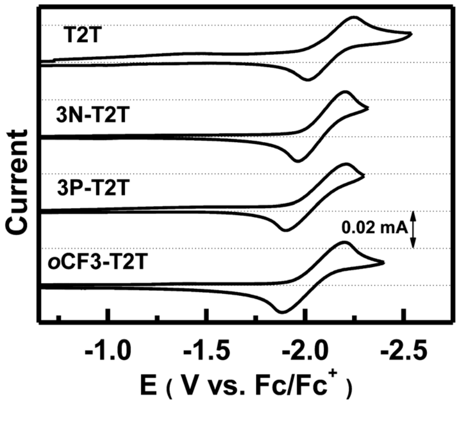

Fig. 2 Cyclic voltammograms of **T2T**, **3N-T2T**, **3P-T2T**, and ***o*CF3-T2T** in THF and 0.1 M $TBAClO_4$ was used as supporting electrolyte. A glassy carbon electrode was used as the working electrode; scan rate 100 mV s^{-1}.

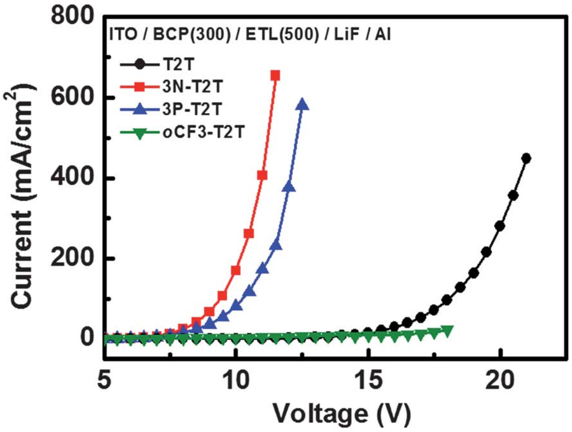

Fig. 3 Current density–voltage (*I*–*V*) characteristics of electron-only devices.

advantageous for the electron-transport properties of the bulk material over electron-withdrawing groups such as CF_3.

Electroluminescent properties

We employed a relatively simple configuration for fabricating OLED devices: ITO/polyethylene dioxythiophene: polystyrene sulfonate (PEDOT:PSS, 30 nm)/4,4′-bis[*N*-(1-naphthyl)-*N*-phenyl]biphenyldiamine (NPB, 20 nm)[11]/4,4′,4′′-tri(*N*-carbazolyl)-triphenylamine (TCTA, 5 nm)[12]/1,3,5-triazine: dopant (25 nm)/1,3,5-triazine (50 nm)/LiF (0.5 nm)/Al; NPB/TCTA functioned as the HT layers, while the 1,3,5-triazine-based compound functioned as the host and ET materials. Four phosphors: blue [bis(4,6-difluorophenyl)-pyridinato-*N*,$C^{2'}$]iridium(III)picolinate (FIrpic),[13] green bis(2-phenylpyridinato)iridium(III)(acetylacetonate) [$(PPy)_2Ir(acac)$],[14] orange bis(2-phenylbenzothiazolato)iridium(III)(acetylacetonate) [$(Bt)_2Ir(acac)$],[15] and red $(Mpq)_2Ir(acac)$,[16] respectively, are used in this study (Scheme 2). A larger energy gap between the HOMO energy levels of TCTA (−5.6 eV) and 1,3,5-triazine (−6.67 to −6.82 eV) suggests that holes would be injected from TCTA into the dopants directly (Scheme 2). The electrons injected from the 1,3,5-triazine layer were trapped by the dispersed dopants, recombining with the holes to generate excitons. The high triplet energy of the host allows the efficient confinement of the emissive excitons within the emissive layer.

The performance of green phosphorescent devices (devices **G1–G4**) made up of $(PPy)_2Ir(acac)$ doped in host **T2T**, **3N-T2T**, **3P-T2T** and ***o*CF3-T2T** used as the emitting layer, respectively, were examined. Fig. 4 shows the current density–voltage–brightness (*J*–*V*–*L*) characteristics and efficiency *versus* brightness of these devices, and the EL data are summarized in Table 2. As shown in Fig. 4(a), the operating voltages of the devices based on **3N-T2T (G2)** and **3P-T2T (G3)** are much lower than those of the devices based on **T2T (G1)** and ***o*CF3-T2T (G4)**, which are consistent with the electron-only device results observed in Fig. 3. The operating voltage at 1000 cd m^{-2} of device **G2** (3.5 V) is slightly lower than that of the device **G3** (4.3 V). Moreover, device **G2** achieved a maximum brightness (L_{max}) of 97 600 cd m^{-2} at 7 V, a maximum external quantum efficiency (η_{ext}) of 11.3% corresponding to a current efficiency (η_c) of 42.3 cd A^{-1} and a maximum power efficiency (η_p) of 42.2 lm W^{-1}, while device **G3** showed a L_{max} of 103 700 cd m^{-2} at 9.5 V, a maximum η_{ext} of 15.7% corresponding to η_c of 56.6 cd A^{-1} and a maximum η_p of 71.6 lm W^{-1} (Table 2). The higher electron injection/transportation properties for **3N-T2T** may be the reason leading to the lower device performances because of the poor charge balance in the emissive layer. The low operating voltage can be attributed to the introduction of pyridine or pyrazoline as the peripheries of the 1,3,5-triazine core, giving a low-lying LUMO level. In addition, coordination effects between the pyridine or pyrazoline peripheries and the Li cations may further reduce their LUMO levels at the interface of the ETL and cathode, giving excellent electron injection and thus reducing the operating voltages.[17] Furthermore, the operating voltages of conventional PhOLEDs can be reduced by using a well-designed ET-type host (functions both as host and ETL) to lower the electron injection barriers (EML/ETL) without using complicated p–i–n junction techniques.

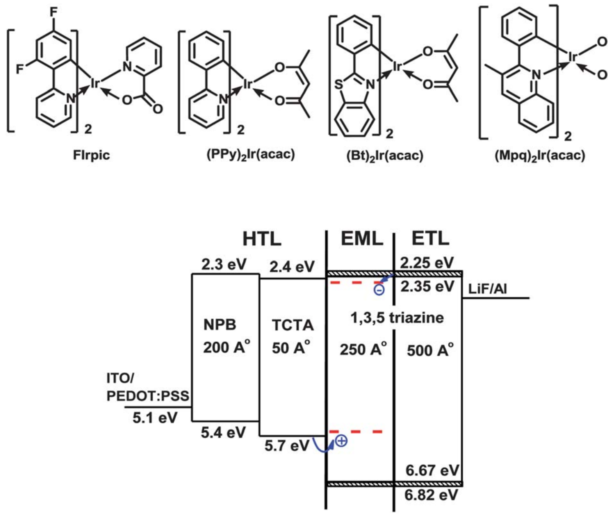

Scheme 2 Molecular structures of the dopants used in this study and an energy level diagram of the device.

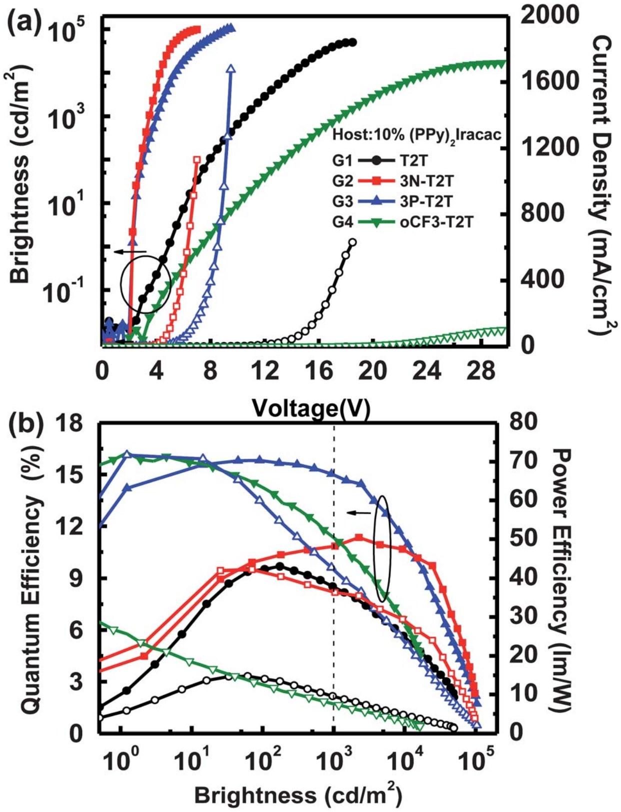

Fig. 4 (a) *J*–*V*–*L* characteristics and (b) plots of EL efficiency *versus* brightness for host: $(PPy)_2Ir(acac)$ devices.

In addition, green PhOLEDs, **3N-T2T**, **3P-T2T** and ***o*CF3-T2T** were also applied in different dopants (from sky blue to red). The triplet energies of **3N-T2T** ($E_T = 2.82$ eV), **3P-T2T** ($E_T = 2.80$ eV) and **3P-T2T** ($E_T = 2.79$ eV) are higher than that of the sky blue phosphor FIrpic ($E_T = 2.62$ eV) and other long-wavelength phosphorescent dopants, implying effective confinement of the triplet excitons on the guest by preventing the reverse

Table 2 EL performance of devices as a function of the host and emitter

	Host: 10% dopant[b]	V_{on}[c]/V	L_{max}/cd m^{-2}	I_{max}/mA cm^{-2}	η_{ext}/%	η_{ext} at 10^3 nit/%	η_c/cd A^{-1}	η_P/lm W^{-1}	CIE1931 (*x*, *y*)
G1[a]	**T2T**: $(PPy)_2$Iracac	2	49 500 (18 V)	630	9.7	8.5 (10.5 V)	36.3	14.7	0.32, 0.64
B2	**3N-T2T**: FIrpic	2	21 900 (7.25 V)	600	8.3	8.2 (3.6 V)	21.3	20.0	0.22, 0.45
G2	**3N-T2T**: $(PPy)_2$Iracac	2	97 600 (7 V)	1130	11.3	10.8 (3.5 V)	42.3	42.2	0.34, 0.62
Y2	**3N-T2T**: $(Bt)_2$Iracac	2	62 300 (7 V)	1160	10.4	10.2 (3.6 V)	27.8	28.8	0.53, 0.47
R2	**3N-T2T**: $(Mpq)_2$Iracac	2	16 000 (7.25 V)	1030	7.7	7.6 (3.8 V)	8.8	10.8	0.65, 0.35
W2	**3N-T2T**: FIrpic + 0.5%$(Mpq)_2$Iracac	2	25 700 (7.5 V)	1090	9.9	9.9 (3.5 V)	16.3	16.9	0.37, 0.41
B3	**3P-T2T**: FIrpic	2	48 800 (9.5 V)	2250	8.0	7.8 (3.7 V)	21.0	19.1	0.29, 0.48
G3	**3P-T2T**: $(PPy)_2$Iracac	2	103 700 (9.5 V)	1680	15.7	15 (4.1 V)	56.6	71.6	0.34, 0.62
Y3	**3P-T2T**: $(Bt)_2$Iracac	2	79 800 (10.25 V)	2100	16.9	16.5 (4.1 V)	41.6	45.8	0.53, 0.47
R3	**3P-T2T**: $(Mpq)_2$Iracac	2	23 700 (12.5 V)	1800	16.4	13.7 (4.6 V)	15.8	20.0	0.66, 0.34
W3	**3P-T2T**: FIrpic + 0.5%$(Mpq)_2$Iracac	2	45 100 (10 V)	1900	10.8	10.5 (3.7 V)	22.3	23.2	0.40, 0.41
B4	***o*CF3-T2T**: FIrpic	3	4970 (29 V)	220	9.7	2.6 (20 V)	20.5	13.9	0.20, 0.35
G4	***o*CF3-T2T**: $(PPy)_2$Iracac	3	16 600 (29.5 V)	100	16.3	11.4 (17.5 V)	61.1	32.6	0.32, 0.64
Y4	***o*CF3-T2T**: $(Bt)_2$Iracac	3	11 600 (30 V)	120	12.4	9.3 (18.5 V)	33.7	13.9	0.52, 0.48
R4	***o*CF3-T2T**: $(Mpq)_2$Iracac	3	2200 (29.5 V)	130	7.5	2.7 (23.5 V)	8.7	3.6	0.64, 0.35

[a] The notation 1–4 indicates the devices fabricated with host materials of **T2T**, **3N-T2T**, **3P-T2T** and ***o*CF3-T2T**, respectively. [b] Device configuration: ITO/PEDOT:PSS (30 nm)/NPB (20 nm)/TCTA (5 nm)/host: dopant (25 nm)/host (50 nm)/LiF (0.5 nm)/Al (100 nm). [c] Turn-on voltage at a brightness of 10^{-2} cd m^{-2}.

energy transfer from the guest to the host. Fig. 5 and 6 depict the current density–voltage–luminance (*J*–*V*–*L*) characteristics, device efficiencies, and EL spectra of the devices incorporating **3N-T2T** and **3P-T2T**, respectively. Table 2 summarizes the electroluminescence data obtained. All of the devices in this study exhibited a low turn-on voltage of 2 V (defined as the voltage at a brightness of 10^{-2} cd m^{-2}). The devices hosted by **3N-T2T** with different dopants still exhibited significantly lower operating voltages than that of **3P-T2T**.

The performances of the FIrpic-based sky blue devices were then examined. In the blue devices, device **B2** based on **3N-T2T** showed a L_{max} of 21 900 cd m^{-2} at 7.25 V (600 mA cm^{-2}), a maximum η_{ext} of 8.3% corresponding to η_c of 21.3 cd A^{-1} and η_P of 20 lm W^{-1}, while device **B3** based on **3P-T2T** achieved a L_{max} of 48 800 cd m^{-2} at 9.5 V (2250 mA cm^{-2}), a maximum η_{ext} of 8% corresponding to η_c of 21 cd A^{-1} and η_P of 19.1 lm W^{-1} (Table 2). In addition, device **B2** and **B3** at 1000 cd m^{-2} exhibited a rather low operating voltage and still retain a high efficiency of η_{ext} = 8.2% and η_{ext} = 7.8% at 3.6 and 3.7 V, respectively, which are much lower than previously reported values based on FIrpic.[18]

As depicted in Fig. 5(c) and 6(c), electroluminescence (EL) spectra originated from the triplet emission of FIrpic exhibited long tails as compared with the typical emission of FIrpic-based devices. The long tail emission can be attributed to inefficient energy transfer from the host to the blue phosphor and/or blue exciton diffusion to the ETL. To further verify the exciton-confinement behaviour of the host, transient photoluminescence decays of the thin films with 10 wt% FIrpic dispersed in **3N-T2T** and **3P-T2T**, and 10 wt% $(PPy)_2Ir(acac)$ doped into **3P-T2T** were measured (Fig. 7). The emissions of FIrpic-doped **3N-T2T** and **3P-T2T** films are not clear single exponential decays with lifetimes of 1.08 and 1.05 μs, respectively, indicating the possibility of triplet energy transferring from FIrpic to **3N-T2T** or **3P-T2T** in the emissive layer.[19] Hence, the long tail emission may be attributed to exciton diffusion out of the emissive layer toward the electron-transport layer of **3N-T2T** or **3P-T2T** in FIrpic-doped blue phosphorescent OLEDs. In contrast, the **3P-T2T**:$(PPy)_2Ir(acac)$ film clearly exhibits a single exponential decay and a relatively short lifetime of 0.5 μs, indicating that the triplet energy transfer from $(PPy)_2Ir(acac)$ to **3P-T2T** was completely suppressed and the energy was well confined and thus an improved performance of the green phosphorescent OLEDs.

In addition, yellow-emitting PhOLEDs were fabricated using $(Bt)_2Ir(acac)$ as the dopant. Excellent performance of orange electrophosphorescence was achieved for device **Y3**, which displayed substantially higher efficiencies (16.9%, 41.6 cd A^{-1}, and 45.8 ml W^{-1}) than those of device **Y2** (10.4%, 27.8 cd A^{-1}, and 28.8 ml W^{-1}). Moreover, in red devices using $(Mpq)_2Ir(acac)$ as the dopant, the device **R3** also exhibited higher efficiencies (16.4%, 15.8 cd A^{-1}, and 20 lm W^{-1}) relative to that of device **R2** (7.7%, 8.8 cd A^{-1}, and 10.8 lm W^{-1}). It is worth mentioning that the maximum efficiencies in our devices appeared to occur in the more useful brightness range of 100–1000 cd m^{-2}, and low operating voltages (<4.6 V) at 1000 cd m^{-2}. The devices displayed relatively pure emission from green to red without long wavelength emission tails as shown in Fig. 5(c) and 6(c), indicating that **3N-T2T** and **3P-T2T** as ETL can effectively prevent exciton diffusion except the blue ones. Therefore, **3N-T2T** and **3P-T2T** can effectively contribute to give lower operating voltages and higher efficiencies with simpler device structures, in which the host materials also serve as the ETL for multi-colour PhOLEDs. In contrast, all of the devices incorporating ***o*CF3-T2T** as the host exhibited lower power efficiencies (see Fig. S1 in the ESI† and Table 2), which is due to its low electron transport properties.

We also fabricated two-emitter WOLEDs (device **W2** and **W3**) utilizing 10 wt% FIrpic and 0.5 wt% $(Mpq)_2Ir(acac)$ co-doped into either **3N-T2T** or **3P-T2T** as a single emissive layer. The proportion of $(Mpq)_2Ir(acac)$ required to produce balanced white emission in these devices was relatively low because the red emission is from either efficient energy transfer from the blue phosphor or direct exciton formation through charge-trapping on the red dopant.[20] Device **W2** hosted by **3N-T2T** achieved a L_{max} of 25 700 cd m^{-2} at 7.5 V (1090 mA cm^{-2}), and EL efficiencies of 9.9%, 16.3 cd A^{-1}, and 16.9 lm W^{-1}; device **W3** hosted

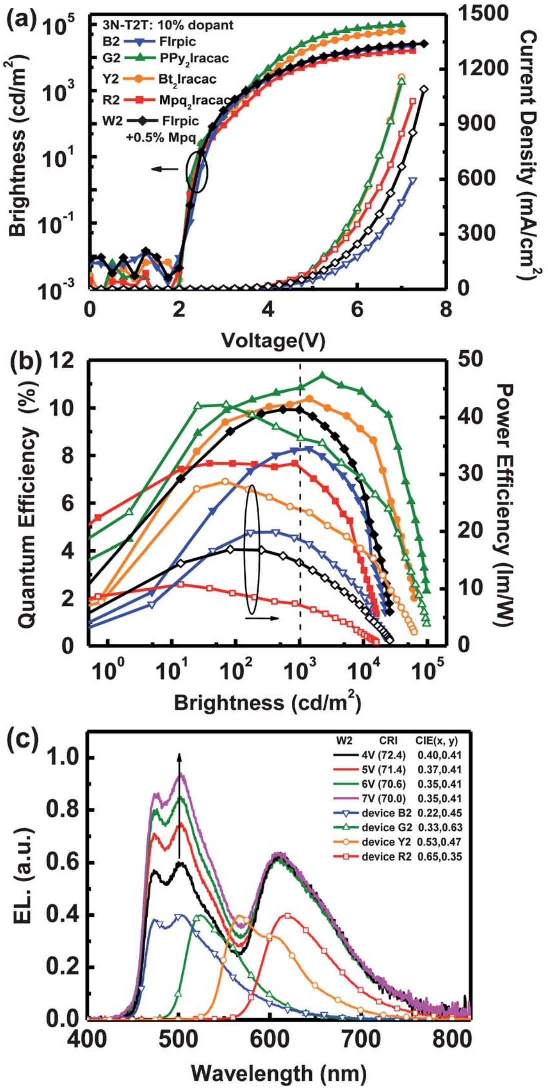

Fig. 5 (a) Current density-voltage-luminance (*J*–*V*–*L*) characteristics, (b) external quantum (η_{ext}) and power efficiencies (η_{P}) as a function of brightness, and (c) EL spectra for devices incorporating **3N-T2T** as host.

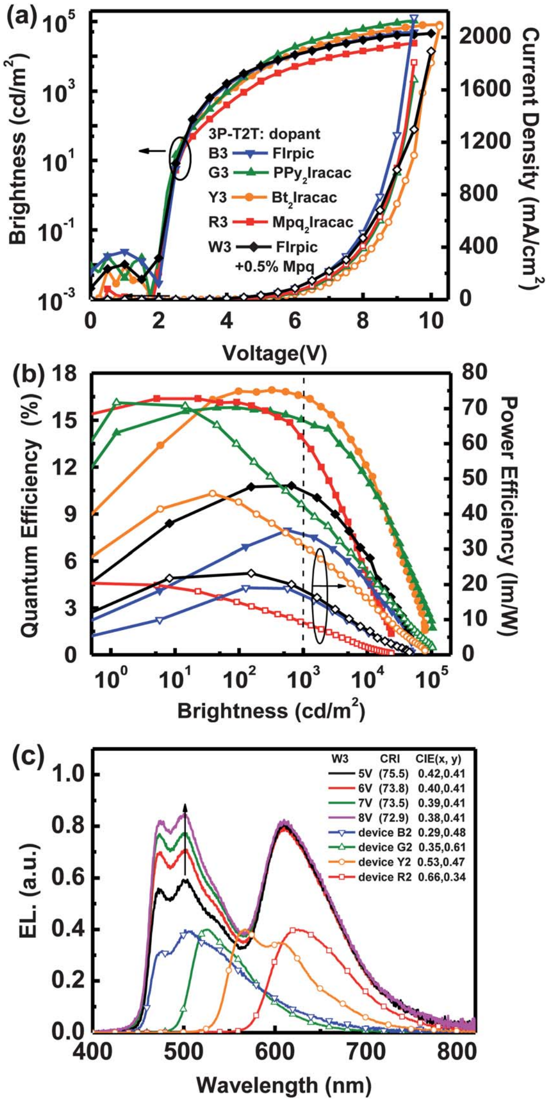

Fig. 6 (a) Current density–voltage–luminance (*J*–*V*–*L*) characteristics, (b) external quantum (η_{ext}) and power efficiencies (η_{P}) as a function of brightness, and (c) EL spectra for devices incorporating **3P-T2T** as host.

by **3P-T2T** achieved a $L_{\max}$ of 45 100 cd m^{-2} at 10 V (1900 mA cm^{-2}), and EL efficiencies of 10.8%, 22.3 cd A^{-1}, and 23.2 lm W^{-1}. The efficiencies of device **W3** were slightly higher than those of the device **W2**, which was probably because device **W3** exhibited a higher ratio of red emission. In addition, when the brightness reached 1000 cd m^{-2}, the efficiencies of devices **W2** and **W3** were still as high as 9.9 (3.5 V) and 10.5% (3.7 V), respectively, with a rather low operating voltage.

Fig. 5(c) and 6(c) depict the EL spectra of device **W2** and **W3** at different operation voltages. As the operation voltage increased, the relative intensity of blue emission increased, leading to a slight shift in the CIE coordinates. This is due to the low concentration of (Mpq)$_2$Ir(acac) in the blend, which results in the partial saturation of emission from (Mpq)$_2$Ir(acac) and the easier formation of blue emission at higher voltage.[21] The EL spectra of devices **W2** and **W3** exhibited main emission peaks at 473, 501 and 610 nm, which were assigned to the emission from FIrpic and (Mpq)$_2$Ir(acac), respectively. Due to the tail emission of FIrpic,

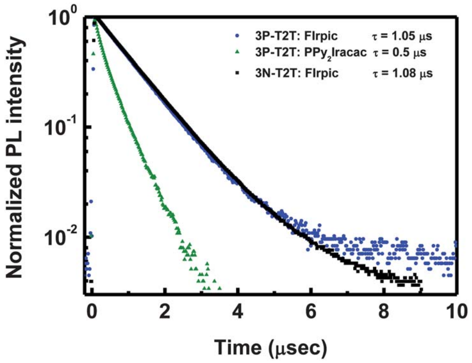

Fig. 7 Transient photoluminescence decay of **3N-T2T** and **3P-T2T**:10 wt% FIrpic as well as **3P-T2T**:10 wt% (PPy)$_2$Ir(acac) under excitation by a nitrogen laser (λ = 337 nm, 10 Hz, 700 ps pulses).

the color-rendering indices (CRI) of devices **W2** and **W3** were calculated to be as high as 75.5–70, which are higher than those of typical two-colour white OLEDs.[22]

Conclusions

In conclusion, we have examined a new series of 1,3,5-triazine-based ET-type host materials containing different polar aromatic groups as the peripheral groups. The relationships between their molecular structures and thermal, electrochemical, and photophysical properties were addressed. Apparently, the introduction of pyridine and pyrazoline as peripheries of 1,3,5-triazine showed excellent electron injection/transport properties, which allow us to adopt a relatively simple device architecture using **3N-T2T** and **3P-T2T** as host and ETL for different color electrophosphorescence devices. These devices exhibited very low operation voltages and achieved high EL efficiencies. For those PhOLEDs, the better efficiency was achieved by using **3P-T2T** to give a maximum η_{ext} of 8%, 15.7%, 16.9%, 16.4% and 10.8% for sky blue (FIrpic), green [$(PPy)_2Ir(acac)$], yellow [$(Bt)_2Ir(acac)$], red [$(Mpq)_2Ir(acac)$] and white [FIrpic+ 0.5 wt%$(Mpq)_2Ir(acac)$], respectively, under the same device structure. Taking advantage of the dual functions of ET-type host materials, PhOLEDs possessing lower operating voltages and high efficiencies with a simpler device structure can be successfully achieved. We believe that our molecular design concept may trigger new ideas for the development of bifunctional host materials, being beneficial for suppressing the production costs of PhOLEDs.

Experimental

Photophysical measurements

Steady state spectroscopic measurements were conducted both in solution and solid films prepared by vacuum (2×10^{-6} torr) deposition on a quartz plate. Absorption spectra were recorded with a U2800A spectrophotometer (Hitachi). Fluorescence spectra at 300 K and phosphorescent spectra at 77 K were measured on a Hitachi F-4500 spectrophotometer upon exciting at the absorption maxima. The experimental values of the HOMO levels were determined with a Riken AC-2 photoemission spectrometer (PES), and those of the LUMO levels were estimated by subtracting the optical energy gap from the measured HOMO. Transient PL decays were measured under excitation by a pulsed nitrogen laser ($\lambda = 337$ nm, 10 Hz, 700 ps pulses) combined with a photomultiplier tube (R928, Hamamatsu) and a synchronous oscilloscope (500 MHz resolution).

OLED fabrications

All chemicals were purified through vacuum sublimation prior to use. The OLEDs were fabricated through vacuum deposition of the materials at 10^{-6} torr onto ITO-coated glass substrates with a sheet resistance of 15 Ω sq^{-1}. The ITO surface was cleaned ultrasonically – sequentially with acetone, methanol, and deionized water – and then it was treated with UV-ozone. The deposition rate of each organic material was *ca.* 1–2 Å s^{-1}. Subsequently, LiF was deposited at 0.1 Å s^{-1} and then capped with Al (*ca.* 5 Å s^{-1}) through shadow mask without breaking the vacuum. The *J*–*V*–*L* characteristics of the devices were measured simultaneously in a glove-box using a Keithley 6430 source meter and a Keithley 6487 picoammeter equipped with a calibration Si-photodiode. EL spectra were measured using a photodiode array (Ocean Optics USB2000).

Acknowledgements

We greatly appreciate the financial support from the National Science Council of Taiwan (NSC 98-2119-M-002-007-MY3 and 100-2112-M-019-002-MY3).

Notes and references

1 M. A. Baldo, D. F. O'Brien, Y. You, A. Shoustikov, S. Sibley, M. E. Thompson and S. R. Forrest, *Nature*, 1998, **395**, 151.

2 S.-J. Su, H. Sasabe, T. I. Takeda and J. Kido, *Chem. Mater.*, 2008, **20**, 1691.

3 (*a*) C. Adachi, R. C. Kwong, P. Djurovich, V. Adamovich, M. A. Baldo, M. E. Thompson and S. R. Forrest, *Appl. Phys. Lett.*, 2001, **79**, 2082; (*b*) R. J. Holmes, S. R. Forrest, Y.-J. Tung, R. C. Kwong, J. J. Brown, S. Garon and M. E. Thompson, *Appl. Phys. Lett.*, 2003, **82**, 2422; (*c*) S. Tokito, T. Iijima, Y. Suzuri, H. Kita, T. Tsuzuki and F. Sato, *Appl. Phys. Lett.*, 2003, **83**, 569; (*d*) K. Goushi, R. Kwong, J. J. Brown, H. Sasabe and C. Adachi, *J. Appl. Phys.*, 2004, **95**, 7798.

4 (*a*) M. A. Baldo, S. Lamansky, P. E. Burrows, M. E. Thompson and S. R. Forrest, *Appl. Phys. Lett.*, 1999, **75**, 4; (*b*) X. Gong, M. R. Robinson, J. C. Ostrowski, D. Moses, G. C. Bazan and A. J. Heeger, *Adv. Mater.*, 2001, **14**, 581; (*c*) S.-J. Yeh, M.-F. Wu, C.-T. Chen, Y.-H. Song, Y. Chi, M.-H. Ho, S.-F. Hsu and C.-H. Chen, *Adv. Mater.*, 2005, **17**, 285; (*d*) K.-T. Wong, Y.-M. Chen, Y.-T. Lin, H.-C. Su and C.-C. Wu, *Org. Lett.*, 2005, **74**, 5361; (*e*) M.-H. Tsai, H.-W. Lin, H.-C. Su, T.-H. Ke, C.-C. Wu, F.-C. Fang, Y.-L. Liao, K.-T. Wong and C.-I. Wu, *Adv. Mater.*, 2006, **18**, 1216; (*f*) P.-I. Shih, C.-L. Chiang, A. K. Dixit, C.-K. Chen, M.-C. Yuan, R.-Y. Lee, C.-T. Chen, E. W.-G. Diau and C.-F. Shu, *Org. Lett.*, 2006, **8**, 2799; (*g*) M.-H. Tsai, Y.-H. Hong, C.-H. Chang, H.-C. Su, C.-C. Wu, A. Matoliukstyte, J. Simokaitiene, S. Grigalevicius, J. V. Grazulevicius and C.-P. Hsu, *Adv. Mater.*, 2007, **19**, 862.

5 S.-J. Su, H. Sasabe, Y.-J. Pu, K. Nakayama and J. Kido, *Adv. Mater.*, 2010, **22**, 3311.

6 (*a*) H. Fukagawa, N. Yokoyama, S. Irisa and S. Tokito, *Adv. Mater.*, 2010, **22**, 4775; (*b*) T.-Y. Hwu, T.-C. Tsai, W.-Y. Hung, S.-Y. Chang, Y. Chi, M.-H. Chen, C.-I. Wu, K.-T. Wong and L.-C. Chi, *Chem. Commun.*, 2008, 4956; (*c*) S. O. Jeon and J. Y. Lee, *Mater. Chem. Phys.*, 2011, **127**, 300; (*d*) S. O. Jeon, K. S. Yook, C. W. Joo and J. Y. Lee, *Appl. Phys. Lett.*, 2009, **94**, 013301; (*e*) J. S. Swensen, E. Polikarpov, A. V. Ruden, L. Wang, L. S. Sapochak and A. B. Padmaperuma, *Adv. Funct. Mater.*, 2011, **21**, 3250; (*f*) Y. D. Sun, L. Duan, D. Q. Zhang, J. Qiao, G. F. Dong, L. D. Wang and Y. Qiu, *Adv. Funct. Mater.*, 2011, **21**, 1881; (*g*) A. Takahashi, A. Endo and C. Adachi, *Jpn. J. Appl. Phys.*, 2006, **45**, 9928.

7 H.-F. Chen, S.-J. Yang, Z.-H. Tsai, W.-Y. Hung, T.-C. Wang and K.-T. Wong, *J. Mater. Chem.*, 2009, **19**, 8112.

8 M. Taillefer, N. Xia and A. Ouali, *Angew. Chem., Int. Ed.*, 2007, **46**, 934.

9 K. Fuchibe and T. Akiyama, *J. Am. Chem. Soc.*, 2006, **128**, 1434.

10 P. I. Djurovich, E. I. Mayo, S. R. Forrest and M. E. Thompson, *Org. Electron.*, 2009, **10**, 515.

11 D.-H. Lee, Y.-P. Liu, K.-H. Lee, H. Chae and S. M. Cho, *Org. Electron.*, 2010, **11**, 427.

12 (*a*) S.-J. Su, E. Gonmori, H. Sasabe and J. Kido, *Adv. Mater.*, 2008, **20**, 4189; (*b*) Y.-Y. Lyu, J. Kwak, W. S. Jeon, Y. Byun, H. S. Lee, D. Kim, C. Lee and K. Char, *Adv. Funct. Mater.*, 2009, **19**, 420.

13 A. F. Rausch, M. E. Thompson and H. Yersin, *J. Phys. Chem. A*, 2009, **113**, 5927.

14 C. Adachi, M. A. Baldo, M. E. Thompson and S. R. Forrest, *J. Appl. Phys.*, 2001, **90**, 5048.

15 S. Lamansky, P. Djurovich, D. Murphy, F. Abdel-Razzaq, R. Kwong, I. Tsyba, M. Bortz, B. Mui, R. Bau and M. E. Thompson, *Inorg. Chem.*, 2001, **40**, 1704.
16 W.-Y. Hung, T.-C. Tsai, S.-Y. Su, K.-T. Wong and L.-C. Chi, *Phys. Chem. Chem. Phys.*, 2008, **10**, 5822.
17 T. Oyamada, H. Yoshizaki, H. Sasabe and C. Adachi, *Chem. Lett.*, 2004, **33**, 1034.
18 S.-J. Su, T. Chiba, T. Takeda and J. Kido, *Adv. Mater.*, 2008, **20**, 2125.
19 M. A. Baldo, C. Adachi and S. R. Forrest, *Phys. Rev. B: Condens. Matter*, 2000, **62**, 10967.
20 (*a*) Y.-H. Niu, Y.-L. Tung, Y. Chi, C.-F. Shu, J. H. Kim, B. Chen, J. Luo, A. J. Carty and A. K.-Y. Jen, *Chem. Mater.*, 2005, **17**, 3532; (*b*) Y. Zhang, F. Huang, Y. Chi and A. K.-Y. Jen, *Adv. Mater.*, 2008, **20**, 1565; (*c*) C.-H. Chien, S.-F. Liao, C.-H. Wu, C.-F. Shu, S.-Y. Chang, Y. Chi, P.-T. Chou and C.-H. Lai, *Adv. Funct. Mater.*, 2008, **18**, 1430.
21 (*a*) Y. Shao and Y. Yang, *Appl. Phys. Lett.*, 2005, **86**, 073510; (*b*) J. Huang, G. Li, E. Wu, Q. Xu and Y. Yang, *Adv. Mater.*, 2006, **18**, 114; (*c*) Q. Wang, J. Ding, D. Ma, Y. Cheng, L. Wang, X. Jing and F. Wang, *Adv. Funct. Mater.*, 2009, **19**, 84.
22 (*a*) C.-H. Chien, F.-M. Hsu, C.-F. Shu and Y. Chi, *Org. Electron.*, 2009, **10**, 871; (*b*) S. Go, Y. Chen, C. Yang, C. Zhong and J. Qin, *Adv. Mater.*, 2010, **22**, 5370; (*c*) H. Sasabe, J. Takamatsu, T. Motoyama, S. Watanabe, G. Wagenblast, N. Langer, O. Molt, E. Fuchs, C. Lennartz and J. Kido, *Adv. Mater.*, 2010, **22**, 5003.